Article

Kinetics of Hg(II) exchange between organic ligands, goethite, and natural organic matter studied with an enriched stable isotope approach

Martin Jiskra, Damian Saile, Jan G. Wiederhold, Bernard Bourdon, Erik Björn, and Ruben Kretzschmar

Environ. Sci. Technol., **Just Accepted Manuscript** • DOI: 10.1021/es503483m • Publication Date (Web): 03 Oct 2014

Kinetics of Hg(II) exchange between organic ligands, goethite, and natural organic matter studied with an enriched stable isotope approach

Martin Jiskra,[†,‡] Damian Saile,[†] Jan G. Wiederhold,[*,†,‡] Bernard Bourdon,[¶] Erik Björn,[§] and Ruben Kretzschmar[†]

Soil Chemistry, Institute of Biogeochemistry and Pollutant Dynamics (IBP), ETH Zurich, CH-8092 Zurich, Switzerland, Isotope Geochemistry, Institute of Geochemistry and Petrology (IGP), ETH Zurich, CH-8092 Zurich, Switzerland, Laboratoire de Géologie de Lyon, ENS Lyon, CNRS and UCBL, Lyon, France, and Department of Chemistry, Umeå University, Sweden

E-mail: wiederhold@env.ethz.ch

[*]To whom correspondence should be addressed
[†]IBP, ETH Zurich
[‡]IGP, ETH Zurich
[¶]ENS Lyon
[§]Department of Chemistry, Umeå University

Abstract

The mobility and bioavailability of toxic Hg(II) in the environment strongly depends on its interactions with natural organic matter (NOM) and mineral surfaces. Using an enriched stable isotope approach, we investigated the exchange of Hg(II) between dissolved species (inorganically complexed or cysteine-, EDTA-, or NOM-bound) and solid-bound Hg(II) (carboxyl-/thiol-resin or goethite) over 30 days under constant conditions (pH, Hg and ligand concentrations). The Hg(II)-exchange was initially fast, followed by a slower phase, and depended on the properties of the dissolved ligands and sorbents. The results were described by a kinetic model allowing the simultaneous determination of adsorption and desorption rate coefficients. The timescales required to reach equilibrium with the carboxyl-resin varied greatly from 1.2 d for $Hg(OH)_2$ to 16 d for Hg(II)-cysteine complexes and approximately 250 d for EDTA-bound Hg(II). Other experiments could not be described by an equilibrium model, suggesting that a significant fraction of total-bound Hg was present in a non-exchangeable form (thiol-resin and NOM: 53-58%; goethite: 22-29%). Based on the slow and incomplete exchange of Hg(II) described in this study, we suggest that kinetic effects must be considered to a greater extent in the assessment of the fate of Hg in the environment and the design of experimental studies, e.g., for stability constant determination or metal isotope fractionation during sorption.

Introduction

Mercury is of great concern for human and ecosystem health due to its ability to be methylated and accumulated along the food chain as toxic methyl-Hg.[1] The mobility and reactivity of Hg(II) in aquatic and terrestrial ecosystems is controlled to a large degree by interactions with dissolved ligands, natural organic matter (NOM), inorganic sulfides, and mineral surfaces.[1–3] A widely used method to assess the bioavailability of Hg is based on a thermodynamic approach, where equilibrium concentrations of dissolved Hg(II)-species (e.g., $HgS^0_{(aq)}$) are calculated.[4] This approach relies on accurate stability constants and the system being at equilibrium, an assumption which has not been thoroughly investigated.[1] Recent findings, suggesting that Hg(II)-species such as Hg(II)-cysteine complexes are actively taken up by bacterial cells,[5–7] or that Hg(II)-(NOM)-sulfide nanoparticles are available for methylation,[8–11] indicate that kinetics have a major effect on the bioavailability of Hg,[12,13] which is not yet fully understood.

Furthermore, many observations on the fate of Hg(II) in experiments and natural systems cannot be explained by thermodynamic approaches. Several studies reported a decrease of labile Hg(II),[14] reducible Hg(II),[15,16] or Hg bioavailability[17] with increasing exposure time of Hg(II) to NOM. These observations were explained by a slow competitive ligand exchange from labile reactive/bioavailable Hg-NOM complexes to strong non-reactive Hg-NOM complexes.[14–17] Hintelmann et al.[18,19] found that Hg(II) newly added to sediments exhibited higher methylation rates than ambient Hg. Jonsson et al.[12,13] reported orders of magnitude different methylation rates depending on the solid/adsorbed phase of Hg(II) and concluded that a combination of thermodynamics and kinetics of Hg(II) dissolution/desorption processes control the methylation and bioavailability of different Hg pools.

Irreversible sorption of Hg(II) and other heavy metals to soils has been described previously[20–23] and was explained by high-affinity binding sites of NOM[21] and lattice or pore diffusion in mineral phases;[21,23] however, the exact mechanisms for the observed sorption hysteresis remained unclear.

These observations raise the question under which conditions purely thermodynamic approaches are justified and where kinetic controls or irreversible sorption play a substantial role for the environmental fate of Hg. Radioisotope and enriched stable isotope approaches were shown to be a powerful tool to investigate exchange kinetics,[24–26] and to assess pool-sizes of exchangeable metals in soils.[27–30] However, measuring isotope exchange kinetics through the activity of radioactive isotopes in solution[24] does not allow distinguishing between isotope exchange and net adsorption, unless the total concentration of the metal in solution is measured with a second analytical technique, often resulting in considerable uncertainties. In contrast, modern mass spectrometry in combination with enriched stable isotopes allows the simultaneous measurement of isotope ratios and concentrations, providing a more reliable approach for distinguishing between isotope exchange and net sorption processes.[30] Here, we present an approach using enriched stable Hg isotopes to simultaneously investigate adsorption and desorption kinetics of Hg(II) with minimized disturbances of the chemical conditions. In a first phase (preconditioning), we sorbed natural abundance Hg to a solid phase. In a second phase (isotope exchange), we replaced the remaining natural abundance Hg in solution by an equal amount of an enriched Hg isotope tracer and investigated the isotope exchange by monitoring the change in isotope ratio in the solution over time. The objectives were (i) to investigate the adsorption and desorption rate coefficients of dissolved inorganically complexed $Hg(II)_{aq}$ or dissolved organic-ligand-bound Hg(II) with solid-bound Hg(II), (ii) to determine the timescales required to reach equilibrium, (iii) to assess the role of ligand type and coordination on the exchange of Hg(II), and (iv) to assess the pool sizes and discuss potential binding mechanisms of non-exchangeable Hg(II).

Experimental Section

Materials and Reagents

All chemicals used in this study were analytical grade and solutions were prepared with ultrapure water (>18.2 MΩ cm, Millipore). Goethite (α-FeOOH), an important iron oxyhydroxide mineral in soils, and two resins with different surface functional groups were used as solid sorbents. The first was a cation exchange resin with carboxyl functional groups on an acrylic polymer backbone (Bio-Rex 70, Bio-Rad). The second was a resin with thiol functional groups on a styrene copolymer backbone (Ambersep GT74, Rohm & Haas). Both resins were in the form of beads with a diameter ranging from 0.3 to 1.2 mm for the carboxyl-resin and from 0.45 to 0.7 mm for the thiol-resin, and they could be easily separated from solution by decantation. The coordination of Hg(II) sorption to thiol-resin has been previously described[31] and this resin was used as model compound for studying sorptive interactions between Hg(II) and organic thiol groups.[31–33] Goethite was synthesized according to a standard procedure (from alkaline solution) by Schwertmann and Cornell[34] and has been used and characterized in previous studies.[35,36,37] The structure of the freeze-dried goethite was verified by X-ray diffraction (XRD) and a N_2-BET specific surface area of 38 $m^2\ g^{-1}$ was determined.[35] Suwannee River NOM (1R101N, IHSS, St. Paul, MN, U.S.) was used as representative for dissolved NOM. Suwannee River NOM has a total sulfur content of 6.5 g kg^{-1}, of which 28% has been reported to be reduced S (S_{red} =56.8 μmol g^{-1}).[38] L-cysteine (Cys, 97%, Aldrich) and ethylenediaminetetraacetic acid (EDTA, 99%, Merck) are low molecular weight (LMW) organic ligands with high affinities for Hg(II),[39,40] occurring in nanomolar to submicromolar concentrations in the environment.[41,42] However, the main reason for choosing cysteine and EDTA as model organic ligands was their wide application in experimental studies and their difference in Hg(II) complexation. Cysteine has been shown to enhance Hg(II) uptake in microorganisms,[5–7] enhance renal toxicity when co-administered with Hg(II)[43] and oxidize Hg(0).[44] EDTA has been extensively used as

competing LMW-ligand for the determination of Hg(II)-NOM stability constants.[45–47] Cysteine forms 1:2-type ($Hg(Cys)_2$) and 1:3-type ($Hg(Cys)_3$) complexes with Hg(II) under the conditions applied in this study.[48,49] Hg(II) is primarily coordinated to the thiol-group and can be further stabilized by the carboxyl-group in the $Hg(Cys)_2$ complex.[49] EDTA forms polydentate complexes with Hg(II) in which Hg is coordinated with carboxyl/amino functional groups (O/N-coordination).[40]

Stock solutions of Hg(II) with natural abundance (NA) isotope composition (NA-Hg) were prepared from a 1000 mg L^{-1} Hg standard solution (Merck). Enriched stable Hg isotope tracers were purchased in oxide form (200-HgO, with 96.41% ^{200}Hg, Oak Ridge National Laboratory) and in metallic form (198-Hg, with 91.75% ^{198}Hg, Trace Sciences International Corp.). Enriched isotope tracer solutions were prepared by dissolution of 200-HgO in 5% HNO_3 and oxidation of metallic 198-Hg with 69% HNO_3 and dilution, respectively. We use the notation "xxx-Hg" for materials or solutions enriched in a specific isotope ^{xxx}Hg. Further information on the exchange resins and enriched Hg isotope tracers are provided in the Supporting Information (SI).

Batch Experiments

Experiments were performed to investigate the isotope exchange between dissolved inorganically complexed Hg(II) ($Hg(II)_{aq}$) and solid-bound Hg(II) (carboxyl-, thiol-resin, or goethite) (Figure 1a) and between Hg(II) complexed to dissolved organic ligands (EDTA, cysteine or NOM) and solid-bound Hg(II) (carboxyl- or thiol-resin) (Figure 1b). All experiments were conducted in 10 mL Teflon centrifuge tubes as individual batch reactors (duplicate for each time-point). The tubes were filled with 9.5 mL sample solution and sealed with Teflon screw caps, leaving a <0.5 mL headspace of air. For carboxyl-, and thiol-resin experiments, performed at pH 4.0 to 4.2, the buffering capacity of the exchange resins was sufficient to maintain a constant pH (±0.05 to ±0.15 pH units). Goethite experiments were less buffered and the suspension pH was 5.4±0.6 and 5.9±0.4 without and with 0.5 mmol L^{-1} chloride,

respectively (Table 1). In the pH range of 4 to 7 and in absence of dissolved organic ligands and chloride, $Hg(II)_{aq}$ was predominantly present in solution as $Hg(OH)_2$ with a minor contribution of cationic Hg species ($HgOH^+$, Hg^{2+}).[50] The pH was chosen for experimental considerations due to the high buffer capacity of the carboxyl-resin at pH 4 and represents typical conditions found in organic-rich terrestrial environments.

In the preconditioning phase (phase **1** in Figure 1) a solution between 1 and 105 μmol L^{-1} of natural abundance NA-Hg(II) was added to carboxyl- and thiol-resins (10 ± 0.2 mg wet mass, 59±2% and 56±2% water content) and goethite (25 ± 1 mg dry mass) (Table 1). The Hg(II) loadings on the carboxyl- and thiol-resins were chosen below the sorption capacity of the resins (Figure S3), to achieve dissolved Hg concentrations of ≈25 nmol L^{-1} after the preconditioning phase. The Hg loadings in this study are higher than expected under environmental conditions, however, they allowed the assessment of the variety of the binding sites, beyond the high-affinity binding sites which are present at low abundances. In experiments with dissolved organic ligands (Figure 1b), those were added simultaneously with the NA-Hg(II) solution and the resins. The suspensions were mixed on an end-over-end shaker at room temperature (23±2 °C) in the dark. Over the preconditioning time of 96 h dissolved NA-Hg(II) was allowed to interact with the dissolved ligands and solid sorbents present, resulting in a decrease in dissolved Hg(II) concentration due to adsorption of Hg(II) to solid phases (Figure S4). After the preconditioning time the solution phase was removed (phase **2** in Figure 1) and the dissolved NA-Hg(II) concentration was measured. The solid-bound Hg(II) fractions (f_{sorbed}) varied between 38% and 99.97% depending on the ligands and sorbents present (Table 1). The solutions of resin-experiments were removed from the resin with a syringe and filtered through a 0.45 μm nylon membrane filter (Perfect-Flow, Wicom). The goethite suspensions were first centrifuged (≈3300 g for 15 min) and then the supernatant was filtered as in the resin experiments. Samples were stabilized with BrCl (0.2M in $HCl_{concd.}$) to 1% (v/v) in solutions without dissolved organic ligands and to 10% (v/v) in solutions with dissolved organic ligands to break down Hg(II)-organic complexes prior to

analysis. Solutions of a 198-Hg isotope tracer were prepared with similar concentrations to the total dissolved NA-Hg measured after the preconditioning phase. When more than 99% Hg was adsorbed, 1% of the total NA-Hg amount was added as 198-Hg because of analytical precision considerations. In these experiments, the higher concentration of 198-Hg at the beginning of the isotopes exchange phase led to a fast initial net adsorption (Figure 3a). In experiments with dissolved organic ligands, solutions with the same ligand concentrations as in the preconditioning phase (Table 1) were mixed with 198-Hg and preconditioned for 96 h prior to addition to the resin. For the isotope exchange experiments the 198-Hg solutions were added to the solid phases (phase **3** in Figure 1). The addition of the 198-Hg solution caused a sudden drop of the $^{202}Hg/^{198}Hg$ isotope ratio (R) in solution, since the dissolved Hg(II) pool was enriched in ^{198}Hg compared to the total Hg in the system. The isotope exchange (phase **4** in Figure 1) between dissolved inorganically complexed 198-Hg(II) (Figure 1a) or 198-Hg(II) complexed to dissolved organic ligands (Figure 1b) and solid-bound NA-Hg(II) was monitored by measuring R in solution over time as it evolved toward the known isotope ratio of the total system (R_{system}). The isotope exchange was stopped after different exchange times (3 h to 30 d) by separating the dissolved and solid pool as described for the preconditioning phase and R and concentration of total dissolved Hg (Hg_{diss}) were measured. To calculate Hg recoveries (Table 1), the solid-bound Hg(II) was desorbed with 5 mL HCl for 24 h (12M for resins and 9M for goethite) and the concentration of Hg(II) sorbed after the exchange phase was measured.

Analytical Methods

Hg_{diss} and R were determined by cold vapor (CV) generation using stannous chloride reduction (HGX-200, Cetac) coupled to a quadrupole inductively coupled plasma mass spectrometer (q-ICPMS; Agilent 7500, Agilent Technologies). All masses were measured in the analog detector mode. Signal intensities were corrected for background by subtraction of the blank signal measured prior to each sample. Data were corrected for instrumental mass

fractionation by applying a linear mass bias correction, calculated from NA-Hg standard measurements performed after every 10 samples. All samples were diluted to Hg concentrations between 0.5 and 25 nmol L^{-1}. The ratio $^{202}Hg/^{198}Hg$ (R) was measured for 45 cycles of 0.6 s and calculated from the background and mass bias corrected ratio of the signal intensities. The analytical precision was tested with artificially spiked standards revealing that this method is capable of resolving 0.005 nM 198-Hg (1% of total Hg) in a 0.5 nM NA-Hg solution (t-test, p= 0.0077), fulfilling the analytical requirements for this study. Hg_{diss} was measured by a reverse isotope dilution approach.[51,52,53,54] A known amount of 200-Hg isotope standard (usually 25 nmol L^{-1}) was added to the samples. Signal intensities of mass 198, 200 and 202 were recorded for 30 cycles of 0.3 s. Concentrations were calculated from instrumental mass bias and background corrected signals applying a matrix inversion approach.[52,54] Hg concentrations of general characterization experiments (sorption isotherms and adsorption kinetics, Figures S3 and S4) were measured using atomic fluorescence spectrometry (CV-AFS; Millenium Merlin, PS Analytical). DOC concentrations were measured using UV absorbance (UV-visible Spectrophotometer, Cary 50, Varian) at 245 nm relative to the NOM stock solution. Proton adsorption and desorption kinetics were measured with a pH electrode.

Data reporting

The total dissolved Hg(II) concentration (Hg_{diss}) was calculated from the concentration of enriched 198-Hg isotope tracer ($C(198\text{-}Hg)_{diss}$) and the concentration of natural abundance Hg ($C(NA\text{-}Hg)_{diss}$).

$$Hg_{diss} = C(198\text{-}Hg)_{diss} + C(NA\text{-}Hg)_{diss} \quad (1)$$

All measured isotope ratios in solution (R) are reported relative to the ratio of the whole

individual batch system (R_{system}):

$$\frac{R}{R_{system}} = \frac{(^{202}Hg/^{198}Hg)_{diss}}{(^{202}Hg/^{198}Hg)_{system}} \quad (2)$$

where $R_{system} = (^{202}Hg/^{198}Hg)_{system}$ is calculated from the amount of Hg ($n(^{202}Hg)_{precond}$ and $n(^{198}Hg)_{precond}$) added as NA-Hg in the preconditioning phase, the amount of Hg ($n(^{202}Hg)_{removed}$ and $n(^{198}Hg)_{removed}$) removed and the amount of Hg ($n(^{202}Hg)_{tracer}$ and $n(^{198}Hg)_{tracer}$) added as 198-Hg in the isotope exchange phase:

$$(^{202}Hg/^{198}Hg)_{system} = \frac{n(^{202}Hg)_{precond} - n(^{202}Hg)_{removed} + n(^{202}Hg)_{tracer}}{n(^{198}Hg)_{precond} - n(^{198}Hg)_{removed} + n(^{198}Hg)_{tracer}} \quad (3)$$

Kinetic modeling

The evolution of R and Hg_{diss} over time during the isotope exchange phase was modeled for ^{202}Hg representing the natural abundance Hg (NA-Hg) remaining in the system and for ^{198}Hg representing the enriched 198-Hg tracer added in the exchange phase. R in solution at time t was calculated following equation 4 where N_{aq}^{202} and N_{aq}^{198} represent the amount (nmol) of ^{202}Hg and ^{198}Hg in solution:

$$R_{aq}(t) = \frac{N_{aq}^{202}(t)}{N_{aq}^{198}(t)} \quad (4)$$

The modeled R is reported relative to the isotope ratio of the system, following the definition described in equation 3. The modeled total dissolved Hg concentration (Hg_{diss}) was calculated as follows:

$$Hg_{diss}^{aq}(t) = \frac{N_{aq}^{202}(t)}{^{202}ab_{NA-Hg}} + \frac{N_{aq}^{198}(t)}{^{198}ab_{198-Hg}} \quad (5)$$

where $^{202}ab_{NA-Hg}$ and $^{198}ab_{198-Hg}$ correspond to the relative abundance of ^{202}Hg in NA-Hg and of ^{198}Hg in the enriched 198-Hg tracer, respectively (Table S2).

The one-pool equilibrium model (model 1a in Figure 2), where dissolved inorganically com-

plexed Hg(II) is exchanging with one pool of solid-bound Hg (Hg(II)-S_1) to equilibrium was described by equations 6 and 7:

$$\frac{dN_{aq}^{202}}{dt} = -k^{ads} \times N_{aq}^{202} + k^{des} \times N_{S1}^{202} \quad (6)$$

$$\frac{dN_{aq}^{198}}{dt} = -k^{ads} \times N_{aq}^{198} + k^{des} \times N_{S1}^{198} \quad (7)$$

where N_{S1}^{202} and N_{S1}^{198} represent the amounts (nmol) of ^{202}Hg and ^{198}Hg sorbed to solid surfaces and k^{ads} and k^{des} are the adsorption and desorption rate coefficients, respectively. Rate coefficients for ^{202}Hg and ^{198}Hg were set to be equal, as kinetic isotope fractionation is not resolvable with the analytical precision used and can be considered insignificant in the framework of this study. The initial conditions of the model were set to the measured experimental conditions at the beginning of the isotope exchange phase (Table S3, details in SI). For experiments with a fast initial isotope exchange followed by a second slower exchange phase, a two-pool model (model 2, Figure 2) with a faster and a slower exchanging sorbed pool provided a better representation of the measured data. In experiments with dissolved organic ligands a model with two dissolved pools exchanging with solid-bound Hg(II) at different rates (model 3, Figure 2) was shown to provide the best fit. The differential equations for the two-pool models which are similar to equations 6 and 7 are provided in the SI. The Hg loading on the solid phases and the pH were not considered in the model and therefore, the rate coefficients are dependent on the experimental conditions.

In cases where R did not approach R_{system}, representing isotopic equilibrium, but reached a plateau at $R/R_{system}<1$, the equilibrium models were not able to describe the experimental results without the presence of an additional non-exchangeable (NE) Hg(II) pool. Potential Hg(II) diffusion into the non-exchangeable pool during the isotope exchange phase was found to have a minor effect on the interpretation of our results (SI). Therefore, the pool size of non-exchangeable Hg(II) was considered constant in size. The pool size of non-exchangeable

solid-bound Hg was described as a fraction of the solid bound NA-Hg(II) (f_{S-NE}) and subtracted from the initial amount of solid-bound NA-Hg(II) for modeling the isotope exchange phase. The pool size of non-exchangeable dissolved organic-ligand-bound Hg(II) (f_{L-NE}) was described accordingly and subtracted from the initial amount of dissolved 198-Hg(II). The adsorption and desorption rate coefficients ($k^{ads1,2}$ and $k^{des1,2}$), pool sizes of non-exchangeable Hg (f_{S-NE} and f_{L-NE}), and the fraction of the faster exchanging pool ($f1$) were simulated using a Monte Carlo approach based on a uniformly distributed pseudorandom number generation in MATLAB (R2012a, MathWorks).[55] The simulations were evaluated based on the sum of squared residuals comparing the model simulations at each experimental time-point with the corresponding measured values. The reported parameters correspond to the best fit, yielding the lowest sum of squared residuals for the measured R and Hg_{diss} for each series. Small differences in the optimal parameters for describing R and Hg_{diss} were found, potentially caused by different analytical procedures or potential mechanisms not considered in the models (e.g., adsorption of Hg-ligand complexes to resin or container wall). The optimization fit for "R only" was taken for an accurate estimation of the timescales to reach equilibrium.

Results and Discussion

Hg(II)-exchange between dissolved inorganic complexes and resins

The isotope exchange between $Hg(II)_{aq}$ and carboxyl-resin-bound Hg(II) was fast, indicated by a rapid increase in R, reaching $R/R_{system}=1$ within less than 4 d (Figure 3b). The results of the $Hg(II)_{aq}$ − carboxyl-resin isotope exchange experiment were well described by the one-pool equilibrium model (model 1a, Figure 2), where one pool of carboxyl-resin-bound Hg(II) exchanges with $Hg(II)_{aq}$ until equilibrium is reached. The Hg(II) adsorption and desorption rate coefficients of the best model fit (Table 2) were considerably lower than for proton sorption (Figure S5). According to the model providing the best fit for R, the

$Hg(II)_{aq}$ − carboxyl-resin system reached equilibrium ($R/R_{system} = 1$) after 1.2 d. The isotope exchange phase between $Hg(II)_{aq}$ and thiol-resin-bound Hg(II) was characterized by a fast initial increase in R followed by a slower increase aproaching a plateau at R/R_{system} ≈0.9 after 16 d, after which it remained constant until the end of the experiment (Figure 3b). A plateau at $R/R_{system}<1$ suggests the presence of a pool of non-exchangeable Hg(II) bound to the thiol-resin. The one-pool model with an additional non-exchangeable pool (1b, Figure 2) and the two pool equilibrium model (2a, Figure 2) poorly matched the results of the $Hg(II)_{aq}$ − thiol-resin experiment (Figure S6). The results were best described by a model with two pools of solid-bound Hg(II) exchanging at different rates and a third pool of non-exchangeable solid-bound Hg(II) (Model 2b, Figure 2), with the fitted parameters given in Table 2. Based on the best model fit, the fast exchanging pool ($f1$) accounted for only ≈0.25% of the total sorbed Hg, however the determined rate coefficients for the fast exchanging pool have to be treated with caution since it was only represented in the first few samples (Table 2). 42% of the total thiol-resin-bound Hg(II) exchanged at slower rates. The remaining 57% were accounted to non-exchangeable Hg(II), corresponding to a Hg(II) loading of 56 nmol mg^{-1} thiol-resin. It is important to realize that a value of 0.9 for R/R_{system} does not correspond to a 90% approach to equilibrium. This is because the pool sizes of dissolved and solid-bound Hg are very different.

Hg(II)-exchange between dissolved organic ligands and carboxyl-resin

The Hg(II)-exchange between the dissolved organic ligands (cysteine and EDTA) and carboxyl-resin was slower as compared to $Hg(II)_{aq}$ (Figures 3c and d). The exchange of Hg-cysteine, where equilibrium was reached after about 2 weeks was considerably faster than the exchange of Hg-EDTA experiment, which did not reach equilibrium within 30 d. We suggest that the faster isotope exchange observed for Hg-cysteine compared to Hg-EDTA was controlled by the different Hg coordination; for Hg-cysteine, mono- or bidentate bonds have to be broken

for Hg(II) to exchange with resin-bound Hg, which has likely a higher probability than the breaking of the polydentate complexation in Hg-EDTA. Whereas one-pool models provided a poor fit, the results of both experimental series with dissolved organic-LMW ligands could be well represented by models with two pools of dissolved organic-ligand-bound Hg(II) (model 3a, Figure 2) with the best-fit parameters given in Table 2.

According to the model fit, the isotope exchange between dissolved Hg-cysteine complexes and carboxyl-resin-bound Hg(II) was in equilibrium after ≈16 d. For the Hg-EDTA experiment, the best-fit model resulted in an equilibration time of ≈250 d; however, this should be interpreted with caution since it represents an extrapolation beyond the duration of our experiments (30 d). The slow isotope exchange of Hg(II)-EDTA complexes is in agreement with previous findings for competitive exchange between Fe(III)-EDTA and Ca(II)-EDTA.[56] In comparison, the predicted timescale for Hg(II)-EDTA complexes to reach equilibrium with carboxyl-resin-bound Hg(II) of ≈250 d would be about twice as long as for the Ca(II)-Fe(III)-EDTA system in solution.

Hg(II)-exchange between dissolved NOM and resins

The isotope exchange between dissolved NOM-bound Hg(II) and Hg(II) bound to carboxyl- or thiol-resin (Figure 3f) was even slower than that observed for the experiments with dissolved LMW-organic ligands and equilibrium was not reached within 30 d, in agreement with previous observations.[57] The isotope ratio in solution of the Hg(II)-NOM experiment with carboxyl-resin reached a plateau at R/R_{system} ≈0.6 after about two weeks, suggesting the presence of non-exchangeable Hg(II). Since Hg(II) bound to carboxyl-resin was reversible in the absence of dissolved organic ligands, this suggests that NOM contained a pool of non-exchangeable Hg(II). NOM in competition with the thiol-resin had a lower Hg(II) loading (4.2 nmol Hg mg^{-1} NOM) compared to NOM in competition with the carboxyl-resin (24 nmol Hg mg^{-1} NOM), which has a lower affinity for Hg(II) than the thiol-resin. The dissolved Hg concentration decreased in both experimental series during the initial isotope exchange

phase (Figure 3e), concomitant with a 15% decrease in NOM concentration relative to the initial NOM over the course of the experiment (Figure S7), indicating possibly adsorption of Hg(II)-NOM complexes to the resins, as described previously.[58] Since the total analytical recovery of Hg in the experimental series with NOM was relatively poor (71% for the NOM-carboxyl series and 81% for the NOM-thiol series, Table 1), we cannot exclude some loss of Hg from these systems, potentially through reduction of Hg(II) to Hg(0) by NOM,[59,60] although our experiments were conducted under oxic conditions in the dark. Model simulations considering the potential loss of Hg (using recovered Hg as initial condition, Figure S8) did not reveal any relevant difference for the interpretation of the results. The results of the isotope exchange were best represented by a model with two exchangeable pools of ligand-bound Hg(II) and one additional pool of non-exchangeable Hg(II)-NOM complexes (model 3b, Figure 2). According to the best-fit model, 53% of the dissolved Hg(II)-NOM complexes in competition with the thiol-resin and 58% in competition with the carboxyl-resin were non-exchangeable, corresponding to 2.2 and 14 nmol Hg(II) per mg Suwannee River NOM for the thiol- and carboxyl-resin experiment, respectively. This implies that between 4.4 to 28 nmol mg^{-1} thiol groups per Suwannee River NOM (assuming a 2:1 thiol:Hg complexation[31]) are capable of complexing Hg(II) irreversibly. This value is in agreement with the 11 - 17 nmol mg^{-1} high affinity binding sites, calculated from the spectroscopic quantification of reduced sulfur (S_{red}) in Suwannee River NOM,[38] based on the assumption that 20 - 30% of the S_{red} is present as thiol.[31] Also Haitzer et al.[61] calculated a concentration of 5 nmol mg^{-1} high affinity binding sites in NOM, however, a recent study using a fluorescent probe equilibrated for 2 hours quantified a thiol-content of 0.7 nmol mg^{-1} in Suwannee River NOM.[62] The non-exchangeable Hg(II)-binding to NOM as compared to Hg(II)-cysteine, where we observed an isotope exchange equilibrium after 16 d, though in both ligand complexes Hg(II) is bound to thiol-groups, could potentially be explained by the difference in coordination of Hg(II). Whereas Hg(II) forms monodentate thiol complexes with cysteine, Hg(II) in NOM is associated to at least two thiol groups[31] and forms bidentate complexes, likely exhibiting a slower

exchange rate than monodentate complexes. The additional complexation of Hg(II) in NOM by a third thiol-group, previously suggested by spectroscopic evidence[31,63] as well as from deprotonation characteristics[64] would further promote this effect. Support for this concept can be derived from the experiment with Hg(II)-EDTA complexes, where the polydentate Hg(II)-binding by EDTA strongly reduced the exchange with the carboxyl-resin. Steric hindrance of the large NOM molecules could potentially further slow down the exchange of Hg-NOM.

Hg(II)-exchange between dissolved inorganic complexes and goethite

The isotope exchange of both experimental series without and with 0.5 mM chloride was initially fast followed by a slower exchange phase reaching a plateau at R/R_{system} ≈0.8 after 12 d (Figures 3g and h). In the presence of chloride, dissolved Hg(II) occurs as chloro complexes (e.g., $HgCl_2$),[50] previously shown to reduce Hg(II) sorption to goethite.[65,37] Chloride was further shown to favor the formation of ternary monodentate Hg(II) surface complexes on goethite, whereas in the absence of chloride bidentate Hg(II) surface complexes where shown to dominate.[66,67] The variations in total Hg concentrations over the course of the experiments (Figure 3g) were probably caused by pH instabilities (Table 1) because the system was not buffered. Preliminary experiments at pH 7 with a 3-morpholinopropanesulfonic acid (MOPS) buffer showed a continuous net adsorption over the 30 d experiment, as previously reported,[37,68] and the isotopic exchange characteristics and the non-exchangeable Hg(II) sorption to goethite was in agreement with the unbuffered data presented here (Figure S9). The results of the isotope exchange phase for both goethite experiments were best described by a model with two exchanging pools (model 2b, Figure 2) of goethite-sorbed Hg(II) (presumably a fast outer-sphere complex pool and slower inner-sphere complex pool) and one pool of non-exchangeable Hg(II). Thereby the sorption rate coefficients of the fast exchanging pool have to be treated with caution since the fast initial phase was poorly covered by the sampling scheme. The model results for the experiment without chloride revealed that 29%

of the total Hg(II) sorbed to goethite was non-exchangeable, corresponding to 0.19 nmol Hg mg^{-1} goethite (5.0 nmol m^{-2} surface area). The experimental series with 0.5 mM chloride was modeled with an non-exchangeable pool of 22%, corresponding to a non-exchangeable pool of 0.1 nmol Hg mg^{-1} goethite (2.8 nmol m^{-2}). This suggests that, although different Hg(II) complexes were described in the presence of chloride (monodentate) compared to without chloride (bidentate),[66,67] there were only minor effects of chloride on the amount of non-exchangeable Hg(II). The diffusion into pores of the goethite appeared to be the most probable cause for the observed non-exchangeable pool of Hg(II), since incorporation of Hg(II) into the lattice structure can be excluded for metals with large ionic radii.[23]

Implications of Exchange Kinetics for Laboratory Experiments

The time required to reach equilibrium is an essential parameter for the design of experiments considered as thermodynamically-controlled, e.g., for the determination of sorption isotherms[69] or stability constants.[47,46,70,45,33] Hg(II) has a high affinity for reduced sulfur and was found to be complexed in NOM with two thiol groups at low Hg/NOM ratios, whereas at higher Hg/NOM ratios the coordination of Hg(II) to C/N-atoms was found to dominate.[31] Accordingly, the apparent stability constant (K) for Hg(II) complexation with NOM was shown to decrease with increasing Hg/NOM ratio, suggesting different binding sites in NOM exhibiting different binding affinities for Hg(II).[45] Assuming a 1:2 complexation of Hg(II) with organic thiol-groups in NOM ($Hg^{2+} + 2\ L^- = HgL_2$), log K values between 28.5 and 40.4 were reported.[33,46,61,64] Studies determining the stability constant of Hg(II)-NOM complexes typically applied equilibration times between 12 h and 13 d,[33,45–47,61,64,70] however the justification for the chosen equilibration times remained arguable.

Our isotope exchange data suggest that equilibration times chosen in many of the previous experiments may have been too short to reach equilibrium. The observation of a positive correlation of stability constants with equilibration times applied in previous studies (Figure S10) supports this argument. Short equilibration times would have the consequence that

Hg(II) is partially associated with low affinity binding sites, e.g., carboxyl groups, which are more abundant than high affinity thiol groups and therefore the probability of Hg(II) to first interact with carboxyl groups is higher. This effect, caused by long timescales required for Hg(II) to exchange to the thermodynamically more stable thiol groups, would reduce the observed stability constant similar to the effect observed by increasing the Hg/DOC ratio.[45] These findings suggest that higher stability constants of the reported range (LogK (HgL_2) = 28.5 - 40.4) are probably more representative for Hg(II) binding to thiol-groups in NOM. This would be in agreement with the previous suggestion that Hg complexation by NOM could be modeled by stability constants for LMW thiol complexes[71] (e.g. for cysteine: logK = 42.7, $Hg^{2+} + 2\ L^{2-} = HgL_2^{2-}$, I = 1M).[39]

Implications for Isotope Fractionation Experiments

The investigation of natural Hg isotope variations in environmental samples has a great potential for studying sources and transformation processes in biogeochemical Hg cycling. To interpret Hg isotope signatures of field samples, it is essential to understand the underlying mechanisms causing the observed variations by stable isotope fractionation.[72] Here, we showed that a considerable fraction of Hg(II) was irreversibly bound to thiol-resin, NOM and, goethite with respect to isotope exchange on the investigated timescales of up to one month. In previous studies investigating Hg isotope fractionation during sorption of Hg(II) to thiol-resin[32] and goethite,[37] preconditioning times between 18h and 30d were employed. Similar timescales have been applied in stable isotope fractionation studies investigating the interaction of other metals, such as Cr,[73] Fe,[74] Cu,[75,76] Zn,[77,78] Mo,[79] Cd,[80] Tl,[81] and U[82] with mineral surfaces and NOM. In the case of Hg(II) sorption to goethite, no dependence of isotope fractionation on preconditioning time could be observed.[37] This observation, however, does not imply that the measured isotope signatures represent exclusively equilibrium isotope effects. We suggest that results from isotope fractionation studies between dissolved and sorbed phases, where part of the isotopes are bound to a non-exchangeable pool, are

417 composed of two signals: (i) a kinetic isotope effect from the first initial adsorption to the
418 non-exchangeable pool, and (ii) an equilibrium isotope effect between the dissolved and the
419 exchangeable pool.

420 Based on constant metal concentration and/or isotope signature in solution over time, previ-
421 ous studies concluded that the observed isotope fractionation must derive from an equilibrium
422 isotope effect.[76–79,81,82] We suggest that this argumentation needs to be revisited since the
423 possibility of a kinetic isotope fractionation signal, trapped in a non-exchangeable pool, has
424 not been considered before. In the case of Hg isotope fractionation during sorption of Hg(II)
425 to thiol-resin[32] and to goethite,[37] kinetic isotope effects have presumably played a minor
426 role, since the observed isotope effects were in good agreement with theoretical equilibrium
427 isotope effects calculated for the relevant Hg(II) species in the specific system.

428 Therefore, in order to derive an equilibrium isotope fractionation factor from the isotopic dif-
429 ference between a dissolved and a sorbed pool, it is essential to experimentally show that the
430 investigated system is in isotopic equilibrium. Isotope exchange experiments using enriched
431 isotopes as previously applied[26,74] and presented here represent a suitable method to assess
432 the timescales required to reach equilibrium. Alternatively, the three-isotope method[83,84]
433 employing an enriched spike allows the simultaneous determination of equilibrium fraction-
434 ation factors and timescales needed to reach equilibrium.

435 Finally, this postulated coexistence of two isotopic signals in different sorbed pools needs to
436 be considered in the interpretation of measured metal isotope data from laboratory and field
437 studies.

438 Environmental Implications

439 The finding that Hg(II) can be bound in a non-exchangeable manner to NOM and mineral
440 surfaces, over timescales of months has at least two important implications for the fate of
441 Hg(II) in the environment: (i) systems which are at equilibrium are capable of sequestering
442 Hg(II) over long timescales, in forms that are likely unavailable for uptake into organisms,

and (ii) in systems which are not at equilibrium, Hg(II) associated partially to low-affinity binding sites (e.g., high abundance carboxyl groups in NOM) may exchange rapidly with dissolved Hg(II) and can lead to a higher availability and reactivity of Hg(II) than expected from the thermodynamic stability with high-affinity binding sites in NOM. Environmental changes such as a drop in pH or redox potential and organic matter degradation might result in a higher reactivity of Hg(II) as expected from desorption rates investigated under constant conditions in this study. In conclusion, kinetic constraints have to be considered to a greater extent in future studies investigating and modeling the fate of Hg(II) in natural systems.

Acknowledgments

We thank Kurt Barmettler for technical assistance in the Soil Chemistry laboratory and three anonymous reviewers for their helpful comments. M.J. acknowledges the FIMIN Reseach Network Programme funded by the European Science Foundation for an Exchange Visit Grant. This research was funded by a research grant from ETH Zurich (ETH-15 09-2).

Supporting Information Available

Experimental details, differential equations and initial conditions of models, additional figures and data tables on sorption isotherms, Hg(II) adsorption kinetics during preconditioning phase, proton adsorption, NOM and goethite experiments. This material is available free of charge via the Internet at http://pubs.acs.org.

References

(1) Hsu-Kim, H.; Kucharzyk, K. H.; Zhang, T.; Deshusses, M. A. Mechanisms regulating mercury bioavailability for methylating microorganisms in the aquatic environment: a critical review. *Environ. Sci. Technol.* **2013**, *47*, 2441–2456.

(2) Gabriel, M. C.; Williamson, D. G. Principal biogeochemical factors affecting the speciation and transport of mercury through the terrestrial environment. *Environ. Geochem. Health* **2004**, *26*, 421–434.

(3) Aiken, G. R.; Hsu-Kim, H.; Ryan, J. N. Influence of dissolved organic matter on the environmental fate of metals, nanoparticles, and colloids. *Environ. Sci. Technol.* **2011**, *45*, 3196–201.

(4) Benoit, J. M.; Gilmour, C. C.; Mason, R. P.; Heyes, A. Sulfide controls on mercury speciation and bioavailability to methylating bacteria in sediment pore waters. *Environ. Sci. Technol.* **1999**, *33*, 951–957.

(5) Schaefer, J. K.; Morel, F. M. M. High methylation rates of mercury bound to cysteine by Geobacter sulfurreducens. *Nat. Geosci.* **2009**, *2*, 123–126.

(6) Schaefer, J. K.; Rocks, S. S.; Zheng, W.; Liang, L.; Gu, B.; Morel, F. M. M. Active transport, substrate specificity, and methylation of Hg(II) in anaerobic bacteria. *Proc. Natl. Acad. Sci. U.S.A.* **2011**, *108*, 8714–8719.

(7) Schaefer, J. K.; Szczuka, A.; Morel, F. M. M. Effect of divalent metals on Hg(II) uptake and methylation by bacteria. *Environ. Sci. Technol.* **2014**, *48*, 3007–3013.

(8) Graham, A. M.; Aiken, G. R.; Gilmour, C. C. Dissolved organic matter enhances microbial mercury methylation under sulfidic conditions. *Environ. Sci. Technol.* **2012**, *46*, 2715–2723.

(9) Zhang, T.; Kim, B.; Leyard, C.; Reinsch, B. C.; Lowry, G. V.; Deshusses, M. A.; Hsu-Kim, H. Methylation of mercury by bacteria exposed to dissolved, nanoparticulate, and microparticulate mercuric sulfides. *Environ. Sci. Technol.* **2012**, *46*, 6950–6958.

(10) Graham, A. M.; Aiken, G. R.; Gilmour, C. C. Effect of dissolved organic matter source and character on microbial Hg methylation in Hg-S-DOM Solutions. *Environ. Sci. Technol.* **2013**, *47*, 5746–5754.

(11) Zhang, T.; Kucharzyk, K. H.; Kim, B.; Deshusses, M. A.; Hsu-Kim, H. Net methylation of mercury in estuarine sediment microcosms amended with dissolved, nanoparticulate, and microparticulate mercuric sulfides. *Environ. Sci. Technol.* **2014**, *48*, 9133–9141.

(12) Jonsson, S.; Skyllberg, U.; Nilsson, M. B.; Westlund, P. O.; Shchukarev, A.; Lundberg, E.; Bjorn, E. Mercury methylation rates for geochemically relevant Hg-II species in sediments. *Environ. Sci. Technol.* **2012**, *46*, 11653–11659.

(13) Jonsson, S.; Skyllberg, U.; Nilsson, M. B.; Lundberg, E.; Andersson, A.; Bjorn, E. Differentiated availability of geochemical mercury pools controls methylmercury levels in estuarine sediment and biota. *Nat. Commun.* **2014**, *5*, 4624.

(14) Hsu, H.; Sedlak, D. L. Strong Hg(II) complexation in municipal wastewater effluent and surface waters. *Environ. Sci. Technol.* **2003**, *37*, 2743–2749.

(15) Miller, C. L.; Liang, L. Y.; Gu, B. H. Competitive ligand exchange reveals time dependant changes in the reactivity of Hg-dissolved organic matter complexes. *Environ. Chem.* **2012**, *9*, 495–501.

(16) Miller, C. L.; Southworth, G.; Brooks, S.; Liang, L.; Gu, B. Kinetic controls on the complexation between mercury and dissolved organic matter in a contaminated environment. *Environ. Sci. Technol.* **2009**, *43*, 8548–8553.

(17) Chiasson-Gould, S. A.; Blais, J. M.; Poulain, A. J. Dissolved organic matter kinetically controls mercury bioavailability to bacteria. *Environ. Sci. Technol.* **2014**, *48*, 3153–61.

(18) Hintelmann, H.; Keppel-Jones, K.; Evans, R. D. Constants of mercury methylation and demethylation rates in sediments and comparison of tracer and ambient mercury availability. *Environ. Toxicol. Chem.* **2000**, *19*, 2204–2211.

(19) Hintelmann, H.; Harris, R. Application of multiple stable mercury isotopes to determine the adsorption and desorption dynamics of Hg(II) and MeHg to sediments. *Mar. Chem.* **2004**, *90*, 165–173.

(20) Coughlin, B. R.; Stone, A. T. Nonreversible adsorption of divalent metal ions (Mn^{II}, Co^{II}, Ni^{II}, Cu^{II}, and Pb^{II}) onto goethite: Effects of acidification, Fe^{II} addition, and picolinic acid addition. *Environ. Sci. Technol.* **1995**, *29*, 2445–2455.

(21) Yin, Y. J.; Allen, H. E.; Huang, C. P.; Sparks, D. L.; Sanders, P. F. Kinetics of mercury(II) adsorption and desorption on soil. *Environ. Sci. Technol.* **1997**, *31*, 496–503.

(22) Liao, L.; Selim, H. M.; DeLaune, R. D. Mercury adsorption-desorption and transport in soils. *J. Environ. Qual.* **2009**, *38*, 1608–1616.

(23) Barrow, N. J.; Brümmer, G. W.; Fischer, L. Rate of desorption of eight heavy metals from goethite and its implications for understanding the pathways for penetration. *Eur. J. Soil Sci.* **2012**, *63*, 389–398.

(24) Benes, P.; Picat, P.; Cernik, M.; Quinault, J. M. Kinetics of radionuclide interaction with suspended-solids in modeling the migration of radionuclides in rivers. 1. Parameters for 2-step kinetics. *J. Radioanal. Nucl. Chem.* **1992**, *159*, 175–186.

(25) Ciffroy, P.; Garnier, J. M.; Pham, M. K. Kinetics of the adsorption and desorption of radionuclides of Co, Mn, Cs, Fe, Ag and Cd in freshwater systems: experimental and modelling approaches. *J. Environ. Radioact.* **2001**, *55*, 71–91.

(26) Johnson, C. M.; Skulan, J. L.; Beard, B. L.; Sun, H.; Nealson, K. H.; Braterman, P. S. Isotopic fractionation between Fe(III) and Fe(II) in aqueous solutions. *Earth Planet. Sci. Lett.* **2002**, *195*, 141–153.

(27) Smolders, E.; Brans, K.; Foldi, A.; Merckx, R. Cadmium fixation in soils measured by isotopic dilution. *Soil Sci. Soc. Am. J.* **1999**, *63*, 78–85.

(28) Young, S. D.; Tye, A.; Carstensen, A.; Resende, L.; Crout, N. Methods for determining labile cadmium and zinc in soil. *Eur. J. Soil Sci.* **2000**, *51*, 129–136.

(29) Hamon, R. E.; Parker, D. R.; Lombi, E. Advances in isotopic dilution techniques in trace element research: a review of methodologies, benefits, and limitations. *Adv. Agron.* **2008**, *99*, 289–343.

(30) Sivry, Y.; Riotte, J.; Sappin-Didier, V.; Munoz, M.; Redon, P.-O.; Denaix, L.; Dupré, B. Multielementary (Cd, Cu, Pb, Zn, Ni) stable isotopic exchange kinetic (SIEK) method to characterize polymetallic contaminations. *Environ. Sci. Technol.* **2011**, *45*, 6247–6253.

(31) Skyllberg, U.; Bloom, P. R.; Qian, J.; Lin, C. M.; Bleam, W. F. Complexation of mercury(II) in soil organic matter: EXAFS evidence for linear two-coordination with reduced sulfur groups. *Environ. Sci. Technol.* **2006**, *40*, 4174–4180.

(32) Wiederhold, J. G.; Cramer, C. J.; Daniel, K.; Infante, I.; Bourdon, B.; Kretzschmar, R. Equilibrium mercury isotope fractionation between dissolved Hg(II) species and thiol-bound Hg. *Environ. Sci. Technol.* **2010**, *44*, 4191–4197.

(33) Dong, W.; Bian, Y.; Liang, L.; Gu, B. Binding constants of mercury and dissolved organic matter determined by a modified ion exchange technique. *Environ. Sci. Technol.* **2011**, *45*, 3576–3583.

(34) Schwertmann, U.; Cornell, R. *Iron Oxides in the Laboratory - Preparation and Characterisation*, 2nd ed.; Wiley-VCH: Weinheim, 2000.

(35) Reichard, P. U.; Kraemer, S. M.; Frazier, S. W.; Kretzschmar, R. Goethite dissolution in the presence of phytosiderophores: rates, mechanisms, and the synergistic effect of oxalate. *Plant Soil* **2005**, *276*, 115–132.

(36) Wiederhold, J. G.; Kraemer, S. M.; Teutsch, N.; Borer, P. M.; Halliday, A. N.; Kretzschmar, R. Iron isotope fractionation during proton-promoted, ligand-controlled, and reductive dissolution of goethite. *Environ. Sci. Technol.* **2006**, *40*, 3787–3793.

(37) Jiskra, M.; Wiederhold, J. G.; Bourdon, B.; Kretzschmar, R. Solution speciation controls mercury isotope fractionation of Hg(II) sorption to goethite. *Environ. Sci. Technol.* **2012**, *46*, 6654–62.

(38) Karlsson, T.; Persson, P.; Skyllberg, U. Extended X-ray absorption fine structure spectroscopy evidence for the complexation of cadmium by reduced sulfur groups in natural organic matter. *Environ. Sci. Technol.* **2005**, *39*, 3048–3055.

(39) Stary, J.; Kratzer, K. Radiometric determination of stability-constants of mercury species complexes with L-cysteine. *J. Radioanal. Nucl. Chem.* **1988**, *126*, 69–75.

(40) Anderegg, G. Polynuclear complexes of the EDTA analogues. *Anal. Chim. Acta* **1999**, *394*, 345–352.

(41) Zhang, J. Z.; Wang, F. Y.; House, J. D.; Page, B. Thiols in wetland interstitial waters and their role in mercury and methylmercury speciation. *Limnol. Oceanogr.* **2004**, *49*, 2276–2286.

(42) Stumm, W.; Morgan, J. J. *Aquatic Chemistry: Chemical Equilibria and Rates in Natural Waters*, third ed. ed.; Series: Environmental science and technology; New York, Wiley, 1996.

(43) Zalups, R. K.; Barfuss, D. W. Nephrotoxicity of inorganic mercury co-administered with L-cysteine. *Toxicology* **1996**, *109*, 15–29.

(44) Zheng, W.; Lin, H.; Mann, B. F.; Liang, L.; Gu, B. Oxidation of dissolved elemental mercury by thiol compounds under anoxic conditions. *Environ. Sci. Technol.* **2013**, *47*, 12827–12834.

(45) Haitzer, M.; Aiken, G. R.; Ryan, J. N. Binding of mercury(II) to dissolved organic matter: The role of the mercury-to-DOM concentration ratio. *Environ. Sci. Technol.* **2002**, *36*, 3564–3570.

(46) Black, F. J.; Bruland, K. W.; Flegal, A. R. Competing ligand exchange-solid phase extraction method for the determination of the complexation of dissolved inorganic mercury(II) in natural waters. *Anal. Chim. Acta* **2007**, *598*, 318–333.

(47) Gasper, J. D.; Aiken, G. R.; Ryan, J. N. A critical review of three methods used for the measurement of mercury (Hg^{2+})-dissolved organic matter stability constants. *Appl. Geochem.* **2007**, *22*, 1583–1597.

(48) Jalilehvand, F.; Leung, B. O.; Izadifard, M.; Damian, E. Mercury(II) cysteine complexes in alkaline aqueous solution. *Inorg. Chem.* **2006**, *45*, 66–73.

(49) Watts, J.; Howell, E.; Merle, J. K. Theoretical studies of complexes between Hg(II) ions and L-cysteinate amino acids. *Int. J. Quantum Chem.* **2014**, *114*, 333–339.

(50) Powell, K. J.; Brown, P. L.; Byrne, R. H.; Gajda, T.; Hefter, G.; Sjoberg, S.; Wanner, H. Chemical speciation of Hg(II) with environmental inorganic ligands. *Aust. J. Chem.* **2004**, *57*, 993–1000.

(51) Sargent, M.; Harte, R.; Harrington, C. *Guidelines for Achieving High Accuracy in Isotope Dilution Mass Spectrometry (IDMS)*; The Royal Society of Chemistry, 2002; Vol. 1.

(52) Qvarnstrom, J.; Frech, W. Mercury species transformations during sample pretreatment of biological tissues studied by HPLC-ICP-MS. *J. Anal. At. Spectrom.* **2002**, *17*, 1486–1491.

(53) Hintelmann, H.; Ogrinc, N. In *Biogeochemistry of Environmentally Important Trace Elements*; Cai, Y., Braids, O. C., Eds.; ACS Symposium Series; Amer. Chem. Soc.: Washington, 2003; Vol. 835; pp 321–338.

(54) Larsson, T.; Bjorn, E.; Frech, W. Species specific isotope dilution with on line derivatisation for determination of gaseous mercury species. *J. Anal. At. Spectrom.* **2005**, *20*, 1232–1239.

(55) Voss, J. *An Introduction to Statistical Computing: A Simulation-based Approach*; John Wiley & Sons: United Kingdom, 2014.

(56) Xue, H.; Sigg, L.; Kari, F. G. Speciation of EDTA in natural waters: exchange kinetics of Fe-EDTA in river water. *Environ. Sci. Technol.* **1995**, *29*, 59–68.

(57) Skyllberg, U.; Xia, K.; Bloom, P. R.; Nater, E. A.; Bleam, W. F. Binding of mercury(II) to reduced sulfur in soil organic matter along upland-peat soil transects. *J. Environ. Qual.* **2000**, *29*, 855–865.

(58) Thurman, E. M.; Malcolm, R. L.; Aiken, G. R. Prediction of capacity factors for aqueous organic solutes adsorbed on a porous acrylic resin. *Anal. Chem.* **1978**, *50*, 775–779.

(59) Alberts, J. J.; Schindle, J. E.; Miller, R. W.; Nutter, D. E. Elemental mercury evolution mediated by humic acid. *Science* **1974**, *184*, 895–896.

(60) Gu, B.; Bian, Y.; Miller, C. L.; Dong, W.; Jiang, X.; Liang, L. Mercury reduction and complexation by natural organic matter in anoxic environments. *Proc. Natl. Acad. Sci. U.S.A.* **2011**, *108*, 1479–1483.

(61) Haitzer, M.; Aiken, G. R.; Ryan, J. N. Binding of mercury(II) to aquatic humic substances: Influence of pH and source of humic substances. *Environ. Sci. Technol.* **2003**, *37*, 2436–2441.

(62) Rao, B.; Simpson, C.; Lin, H.; Liang, L.; Gu, B. Determination of thiol functional groups on bacteria and natural organic matter in environmental systems. *Talanta* **2014**, *119*, 240–247.

(63) Nagy, K. L.; Manceau, A.; Gasper, J. D.; Ryan, J. N.; Aiken, G. R. Metallothionein-like multinuclear clusters of mercury(II) and sulfur in peat. *Environ. Sci. Technol.* **2011**, *45*, 7298–7306.

(64) Khwaja, A. R.; Bloom, P. R.; Brezonik, P. L. Binding constants of divalent mercury (Hg^{2+}) in soil humic acids and soil organic matter. *Environ. Sci. Technol.* **2006**, *40*, 844–849.

(65) Barrow, N. J.; Cox, V. C. The effects of pH and chloride concentration on mercury sorption. I. by goethite. *J. Soil Sci.* **1992**, *43*, 295–304.

(66) Kim, C. S.; Rytuba, J. J.; Brown, J., G. E. EXAFS study of mercury(II) sorption to Fe- and Al-(hydr)oxides I. Effects of pH. *J. Colloid Interface Sci.* **2004**, *271*, 1–15.

(67) Kim, C. S.; Rytuba, J.; Brown, J., G. E. EXAFS study of mercury(II) sorption to Fe- and Al-(hydr)oxides - II. Effects of chloride and sulfate. *J. Colloid Interface Sci.* **2004**, *270*, 9–20.

(68) Fischer, L.; Brmmer, G. W.; Barrow, N. J. Observations and modelling of the reactions of 10 metals with goethite: adsorption and diffusion processes. *Eur. J. Soil Sci.* **2007**, *58*, 1304–1315.

(69) Limousin, G.; Gaudet, J. P.; Charlet, L.; Szenknect, S.; Barthes, V.; Krimissa, M. Sorption isotherms: A review on physical bases, modeling and measurement. *Appl. Geochem.* **2007**, *22*, 249–275.

(70) Lamborg, C. H.; Tseng, C. M.; Fitzgerald, W. F.; Balcom, P. H.; Hammerschmidt, C. R. Determination of the mercury complexation characteristics of dissolved organic matter in natural waters with "reducible Hg" titrations. *Environ. Sci. Technol.* **2003**, *37*, 3316–3322.

(71) Skyllberg, U. Competition among thiols and inorganic sulfides and polysulfides for Hg and MeHg in wetland soils and sediments under suboxic conditions: Illumination of controversies and implications for MeHg net production. *J. Geophys. Res.* **2008**, *113*.

(72) Sonke, J. E.; Heimburger, L. E.; Dommergue, A. Mercury biogeochemistry: paradigm shifts, outstanding issues and research needs. *C. R. Geosci.* **2013**, *345*, 213–224.

(73) Ellis, A. S.; Johnson, T. M.; Bullen, T. D. Using chromium stable isotope ratios to quantify Cr(VI) reduction: lack of sorption effects. *Environ. Sci. Technol.* **2004**, *38*, 3604–3607.

(74) Morgan, J. L. L.; Wasylenki, L. E.; Nuester, J.; Anbar, A. D. Fe isotope fractionation during equilibration of Fe-organic complexes. *Environ. Sci. Technol.* **2010**, *44*, 6095–6101.

(75) Bigalke, M.; Weyer, S.; Wilcke, W. Copper isotope fractionation during complexation with insolubilized humic acid. *Environ. Sci. Technol.* **2010**, *44*, 5496–5502.

(76) Ryan, B. M.; Kirby, J. K.; Degryse, F.; Scheiderich, K.; McLaughlin, M. J. Copper isotope fractionation during equilibration with natural and synthetic ligands. *Environ. Sci. Technol.* **2014**, *48*, 8620–8626.

(77) Juillot, F.; Marechal, C.; Ponthieu, M.; Cacaly, S.; Morin, G.; Benedetti, M.; Hazemann, J. L.; Proux, O.; Guyot, F. Zn isotopic fractionation caused by sorption on goethite and 2-lines ferrihydrite. *Geochim. Cosmochim. Acta* **2008**, *72*, 4886–4900.

(78) Jouvin, D.; Louvat, P.; Juillot, F.; Marechal, C. N.; Benedetti, M. F. Zinc isotopic fractionation: why organic matters. *Environ. Sci. Technol.* **2009**, *43*, 5747–5754.

(79) Wasylenki, L. E.; Rolfe, B. A.; Weeks, C. L.; Spiro, T. G.; Anbar, A. D. Experimental investigation of the effects of temperature and ionic strength on Mo isotope fractionation during adsorption to manganese oxides. *Geochim. Cosmochim. Acta* **2008**, *72*, 5997–6005.

(80) Wasylenki, L. E.; Swihart, J. W.; Romaniello, S. J. Cadmium isotope fractionation during adsorption to Mn oxyhydroxide at low and high ionic strength. *Geochim. Cosmochim. Acta* **2014**, *140*, 212–226.

(81) Nielsen, S. G.; Wasylenki, L. E.; Rehkamper, M.; Peacock, C. L.; Xue, Z. C.; Moon, E. M. Towards an understanding of thallium isotope fractionation during adsorption to manganese oxides. *Geochim. Cosmochim. Acta* **2013**, *117*, 252–265.

(82) Brennecka, G. A.; Wasylenki, L. E.; Bargar, J. R.; Weyer, S.; Anbar, A. D. Uranium isotope fractionation during adsorption to Mn-oxyhydroxides. *Environ. Sci. Technol.* **2011**, *45*, 1370–1375.

(83) Matsuhisa, Y.; Goldsmith, J. R.; Clayton, R. N. Mechanisms of hydrothermal crystallization of quartz at 250°C and 150 kbar. *Geochim. Cosmochim. Acta* **1978**, *42*, 173–182.

(84) Frierdich, A. J.; Beard, B. L.; Reddy, T. R.; Scherer, M. M.; Johnson, C. M. Iron isotope fractionation between aqueous Fe(II) and goethite revisited: New insights based on a multi-direction approach to equilibrium and isotopic exchange rate modification. *Geochim. Cosmochim. Acta* **2014**, *139*, 383–398.

696

697

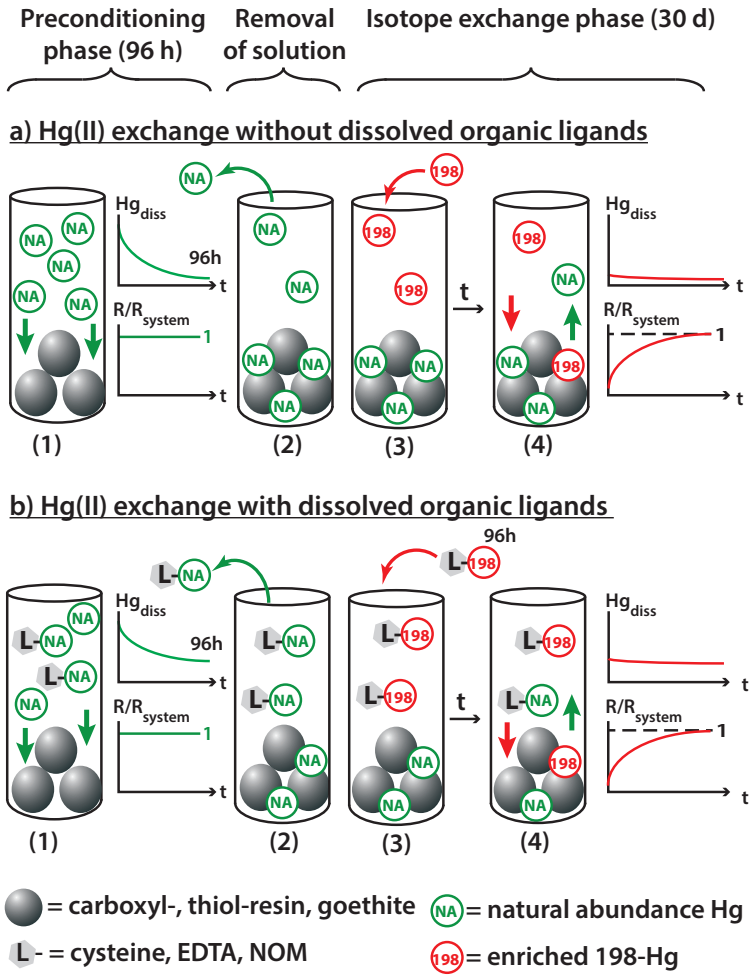

Figure 1: Setup for Hg(II) isotope exchange experiments without dissolved organic ligands **(a)** and with dissolved organic ligands **(b)**. In the preconditioning phase **(1)** natural abundance NA-Hg was mixed with **(a)** solid phases (carboxyl-, thiol-resin or goethite) and **(b)** with dissolved organic ligands (cysteine, EDTA, and Suwannee river natural organic matter (NOM)) and solid phases (carboxyl- and thiol-resin) and allowed to adsorb for 96 h. Then the dissolved NA-Hg(II) species in solution were removed **(2)** and replaced by a similar concentration of enriched 198-Hg(II) isotope tracer **(3)**. The 198-Hg tracer addition caused a sudden drop in the isotope ratio in solution (R) which was normalized to the isotope ratio of the whole system (R_{system}). In the isotope exchange phase **(4)**, the exchange kinetics as expressed by the approach of R towards R_{system} was investigated over 30 d.

Table 1: Parameters of experimental series: Dissolved ligand type and concentration ([L], μmol L^{-1}), solid phase type (C-resin= carboxyl-resin, T-resin= thiol-resin) and concentration ([solid], g L^{-1}), pH, initial NA-Hg concentration ([NA-Hg], μmol L^{-1}) and enriched 198-Hg tracer concentration added for the isotope exchange phase ([198-Hg], μmol L^{-1}), fraction of Hg sorbed after the preconditioning phase (f_{sorb}, %) and total Hg recovery[a], errors are $\pm 1\sigma$.

series	**Dissolved ligand**	**[L]** (μmol L^{-1})	**solid phase**	**[solid]** (g L^{-1})	**pH**	**NA-Hg]** (μmol L^{-1})	**[198-Hg]** (μmol L^{-1})	f_{sorb} (%)	**recovery** (%)
$Hg(II)_{aq}$ – C-resin	no	-	C-resin	1.05	4.0±0.05	9.97	0.094	99.6±0.5	110±5
$Hg(II)_{aq}$ – T-resin	no	-	T-resin	1.05	4.0±0.15	103.20	0.944	99.97±0.004	97±2
Hg(II)-EDTA – C-resin	EDTA	2	C-resin	1.05	4.1±0.05	10.62	1.747	83±2	100±1
Hg(II)-cysteine – C-resin	cysteine	2	C-resin	1.05	4.2±0.12	8.62	0.482	94±0.6	100±2
Hg(II)-NOM – C-resin	SR-NOM	43.9[b]	C-resin	1.05	4.1±0.05	12.22	1.555	83±2	71±6
Hg(II)-NOM – T-resin	SR-NOM	439[b]	T-resin	1.05	4.0±0.08	105.20	2.541	97±0.2	81±2
$Hg(II)_{aq}$ – goethite	no	-	goethite	2.64	5.4±0.6	0.81	0.103	88±7	87±5
Hg(II)-Cl_{aq} – goethite	chloride	500	goethite	2.64	5.9±0.4	0.94	0.624	39±15	100±7

[a] calculated for sum of NA-Hg and 198-Hg

[b] mg NOM L^{-1}

Table 2: Parameters of model fits: model type according to Figure 2, adsorption and desorption rate coefficients (k^{ads1}, k^{ads2}, k^{des1} and k^{des2}), initial size of fast exchangeable pool relative to total exchangeable pool ($f1$), Pool size of non-exchangeable Hg (f_{NE}), time to reach equilibrium (t_{eq}), and coefficient of determination for the isotope ratio fit (R^2 (R)) and the concentration fit (R^2 ($Hg_{dissolved}$)). (C-resin= carboxyl-resin , T-resin= thiol-resin)

series	**model**	$\mathbf{k^{ads1}}$ (h^{-1})	$\mathbf{k^{ads2}}$ (h^{-1})	$\mathbf{k^{des1}}$ (h^{-1})	$\mathbf{k^{des2}}$ (h^{-1})	$\boldsymbol{f1}$ (%)	$\boldsymbol{f_{NE}}$ (%)	$\mathbf{t_{eq}}$ (d)	$\mathbf{R^2}$ **(R)**	$\mathbf{R^2}$ **(Hg_{diss})**
$Hg(II)_{aq}$ – C-resin	1a	7.7×10^{-1}	-	8.2×10^{-4}	-	100	0	$\approx$1.2 [b]	0.972	0.925
$Hg(II)_{aq}$ – T-resin	2b	1.9×10^{-1}	1.0	6.9×10^{-2}	6.0×10^{-4}	0.5	57	$\gg$30 [a]	0.984	0.996
Hg(II)-EDTA – C-resin	3a	2.2×10^{-3}	5.3×10^{-5}	4.3×10^{-2}	2.7×10^{-3}	11	0	$\approx$250 [b,c]	0.989	0.629
Hg(II)-cysteine – C-resin	3a	4.9×10^{-2}	2.8×10^{-4}	3.8×10^{-1}	3.8×10^{-2}	42	0	$\approx$16 [b]	0.994	0.850
Hg(II)-NOM – C-resin	3b	3.3	1.8×10^{-2}	6.7×10^{-3}	6.8×10^{-5}	97	58	$\gg$30 [a]	0.993	0.908
Hg(II)-NOM – T-resin	3b	7.6	7.6×10^{-3}	2.1×10^{-2}	2.2×10^{-5}	90	53	$\gg$30 [a]	0.968	0.872
$Hg(II)_{aq}$ – goethite	2b	5.9×10^{-1}	5.0×10^{-3}	1.4×10^{-1}	2.0×10^{-2}	27	29	$\gg$30 [a]	0.975	0.634
$Hg(II)\text{-}Cl_{aq}$ – goethite	2b	4.6	4.1×10^{-3}	6.7	1.1×10^{-2}	47	22	$\gg$30 [a]	0.962	0.616

[a] no estimation possible based on 30 d exchange experiment.

[b] derived from isotope ratio optimization only (R only)

[c] extrapolated

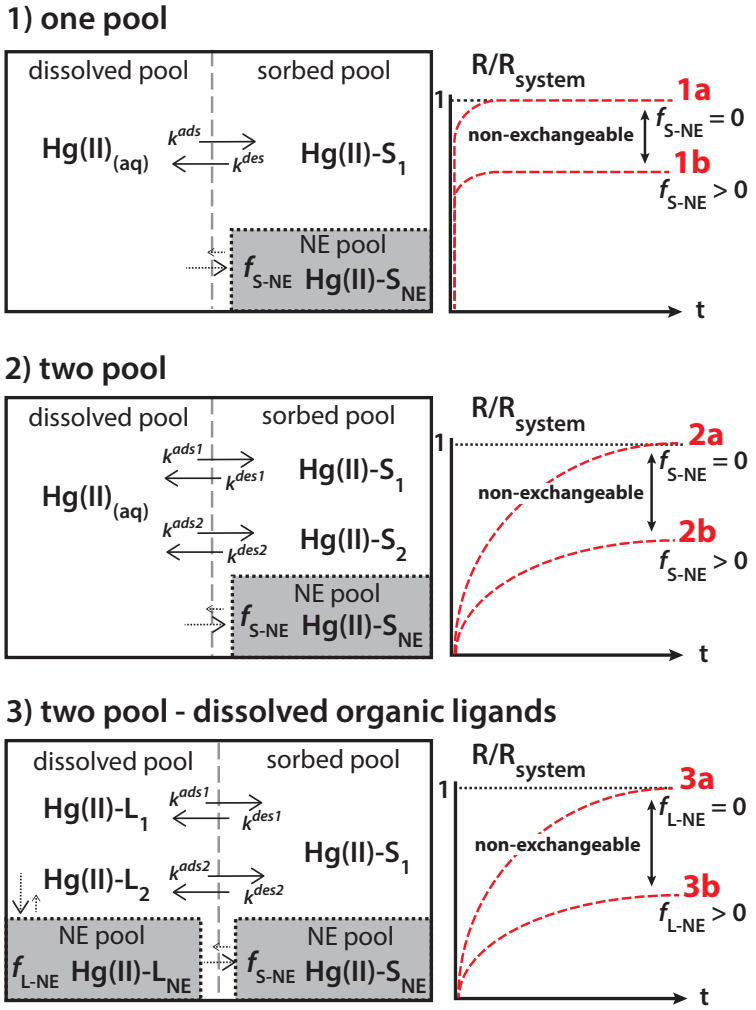

Figure 2: Models describing the isotope exchange phase. In model **1** one pool of inorganically-complexed dissolved $Hg(II)_{(aq)}$ exchanges with one pool of solid-bound Hg(II)-S_1. In model **2** two solid-bound Hg pools (Hg(II)-S_1 and Hg(II)-S_2) are exchanging at different rates with dissolved $Hg(II)_{(aq)}$. In the presence of dissolved organic ligands (model **3**) two dissolved organic-ligand-bound Hg pools (Hg(II)-L_1 and Hg(II)-L_2) are exchanging with one solid-bound pool (Hg(II)-S_1). Isotope exchange experiments approaching equilibrium **(1a, 2a, and 3a)** are characterized by R/R_{system} values approaching 1. Experiments reaching a R/R_{system} plateau below 1 **(1b, 2b, and 3b)** indicate the presence of Hg(II) in a non-exchangeable (NE) pool of solid-bound Hg(II) (f_{S-NE} >0) or for dissolved NOM ligands **(3b)** a non-exchangeable dissolved pool (f_{L-NE} >0). The non-exchangeab pools were considered to be constant in size and not interacting with exchangeable Hg during the isotope exchange phase, after they had been filled in the preconditioning phase.

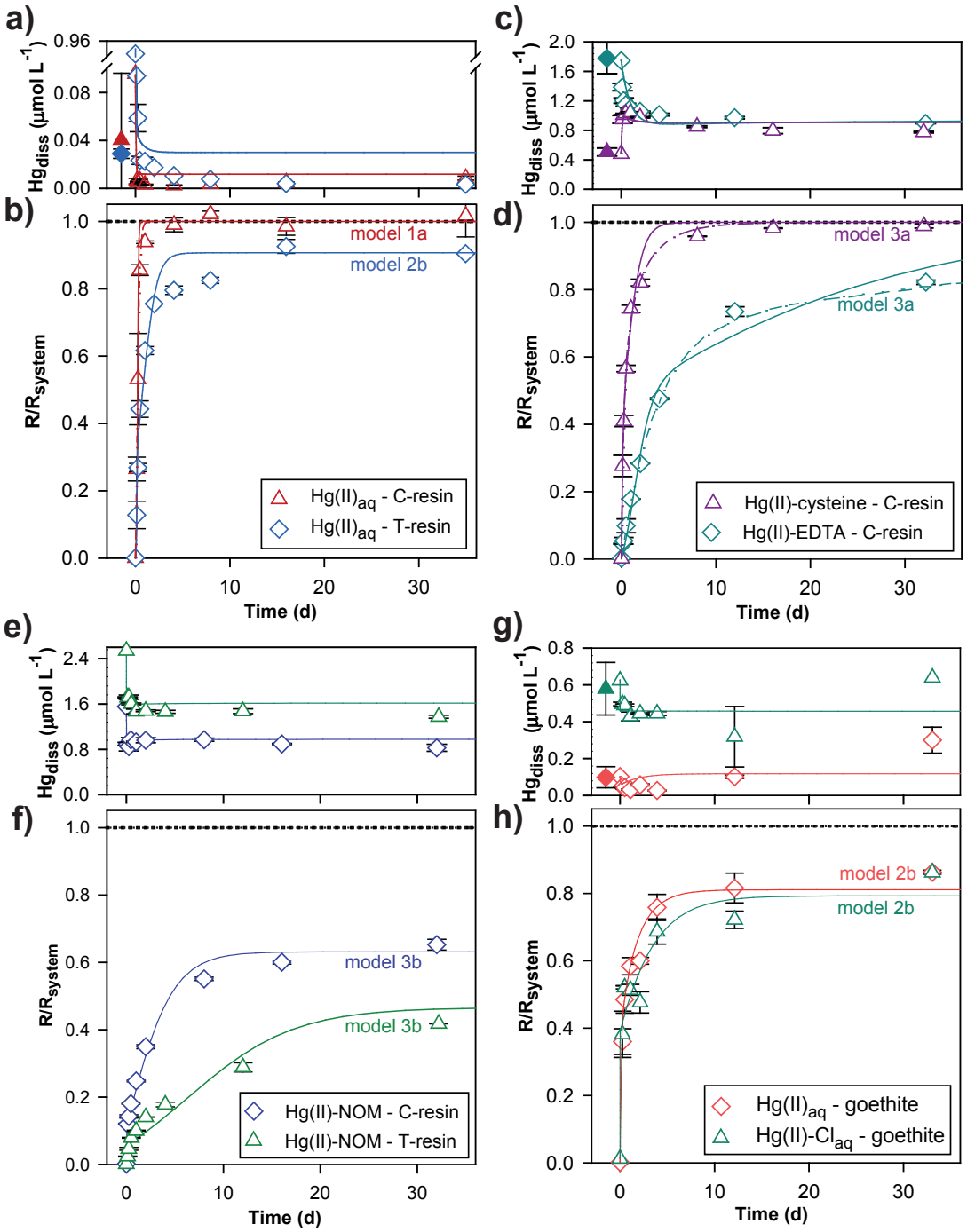

Figure 3: Total dissolved Hg concentration (Hg_{diss}) in μmol L^{-1} and isotope ratio (R/R_{system}) in solution over 30d isotope exchange phase (open symbols) of different experiments: **(a, b)** between $Hg(II)_{aq}$ and carboxyl (C-) or thiol (T-) resin-bound Hg(II), **(c, d)** between dissolved Hg(II)-cysteine or Hg(II)-EDTA and C-resin-bound Hg(II) and, **(e, f)** between dissolved Suwannee River NOM-bound Hg(II) and C- or T-resin-bound Hg(II), and **(g, h)** between $Hg(II)_{aq}$ and Hg(II) sorbed to goethite. Error bars represent the range of duplicate batch experiments for the open symbols (smaller than symbol size if not visible). The solid lines represent the best fits of modeled concentration and isotope ratio (models refer to Figure 2) and dashed lines represent the best fit for the equilibrium timescale determination (R only, see text). The closed symbols represent Hg_{diss} after the 96 h preconditioning phase ($\pm\sigma$).

TOC graph

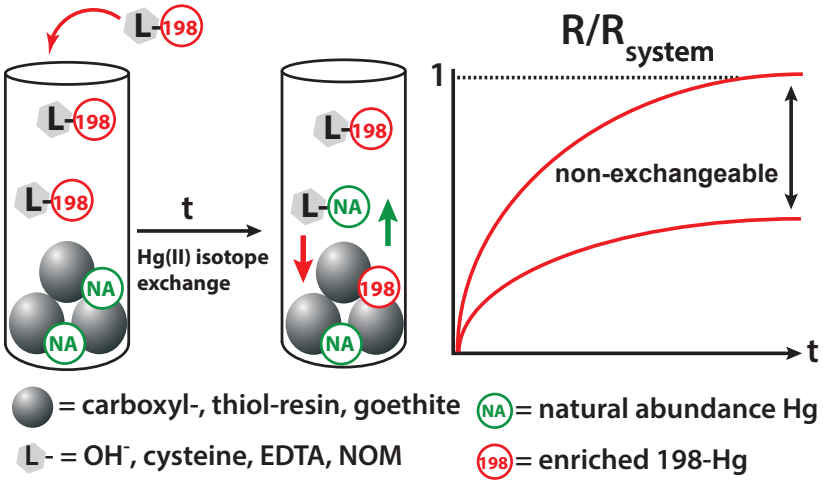
L-198
L-198
L-198
NA
NA
t
Hg(II) isotope exchange
L-198
L-NA
198
NA
R/R system
1
non-exchangeable
t
= carboxyl-, thiol-resin, goethite
L- = OH-, cysteine, EDTA, NOM
NA = natural abundance Hg
198 = enriched 198-Hg